

## Article

# A Ratiometric Fluorescence Probe of Dopamine-Functionalized Carbon Nanodots for Hypochlorite Detection

Wenjing Qi , Lei Chen, Chengpei Du and Yi Wang

Chongqing Key Laboratory of Inorganic Functional Materials, College of Chemistry, Chongqing Normal University, Chongqing 401331, China

\* Correspondence: wenjingqi616@cqnu.edu.cn; Tel.: +86-23-65362777

**Abstract:** A dopamine-functionalized carbon nanodot (C-dots) ratiometric fluorescence probe for hypochlorite ( $\text{ClO}^-$ ) detection is reported. Fluorescent C-dots with maximal emission at 420 nm are synthesized via the hydrothermal synthesis of 3-hydroxyphenylboric acid at 160 °C for 8 h. After modified with dopamine for 5 min, the obtained dopamine-functionalized C-dots exhibit two maximal fluorescence emissions at 420 nm and 460 nm. Fluorescent intensity at 460 nm gets quenched with the addition of  $\text{ClO}^-$  and fluorescent intensity at 420 nm is almost unaffected. Therefore dopamine-functionalized C-dots can be used as ratiometric fluorescence probe for highly sensitive detection of  $\text{ClO}^-$ . The ratio of fluorescent intensity at 460 nm and 420 nm ( $I_{460\text{nm}}/I_{420\text{nm}}$ ) has a linear relationship with the concentration of  $\text{ClO}^-$  from 2  $\mu\text{M}$  to 60  $\mu\text{M}$  and limit of detection (LOD) of 0.6  $\mu\text{M}$ . It shows high selectivity for the detection of  $\text{ClO}^-$  toward other anions ( $\text{SO}_4^{2-}$ ,  $\text{Cl}^-$ ,  $\text{NO}_3^-$ ,  $\text{S}^{2-}$ ,  $\text{CO}_3^{2-}$ ), metal ions ( $\text{Mg}^{2+}$ ,  $\text{Ba}^{2+}$ ,  $\text{Ag}^+$ ,  $\text{Fe}^{3+}$ ,  $\text{Ca}^{2+}$ ,  $\text{Na}^+$ ,  $\text{Cr}^{6+}$ ,  $\text{Cr}^{3+}$ ,  $\text{Hg}^+$ ), or other substances such as  $\text{H}_2\text{O}_2$ , glutamate, cysteine, and citric acid. When it is utilized in  $\text{ClO}^-$  detection in tap water, the average recoveries are from 95.7% to 103.2% with the relative standard deviations (RSDs) lower than 5%.

**Keywords:** dopamine-functionalized carbon nanodot; ratiometric fluorescent probe; hypochlorite ions ( $\text{ClO}^-$ )



**Citation:** Qi, W.; Chen, L.; Du, C.; Wang, Y. A Ratiometric Fluorescence Probe of Dopamine-Functionalized Carbon Nanodots for Hypochlorite Detection. *Chemosensors* **2022**, *10*, 383. <https://doi.org/10.3390/chemosensors10100383>

Academic Editor: Jin-Ming Lin

Received: 22 August 2022

Accepted: 19 September 2022

Published: 22 September 2022

**Publisher's Note:** MDPI stays neutral with regard to jurisdictional claims in published maps and institutional affiliations.



**Copyright:** © 2022 by the authors. Licensee MDPI, Basel, Switzerland. This article is an open access article distributed under the terms and conditions of the Creative Commons Attribution (CC BY) license (<https://creativecommons.org/licenses/by/4.0/>).

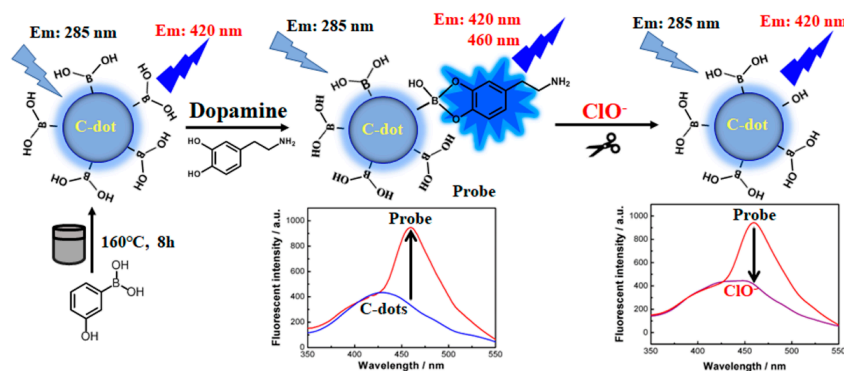
## 1. Introduction

Hypochlorite ( $\text{ClO}^-$ ) is a strong oxidant, which is widely used in wastewater disinfection, deodorization, and other production processes in water treatment. The concentration of  $\text{ClO}^-$  must be strictly controlled because if the concentration of  $\text{ClO}^-$  is too low it cannot effectively kill pathogenic bacteria.  $\text{ClO}^-$  also plays an important role in resisting pathogenic microorganisms and pathogens and viruses in the internal immune system of organisms [1–4]. Once the concentration in biological cells exceeds the normal range, it will cause serious damage to phospholipids, proteins, DNA, and other biological macromolecules, causing a series of lesions in the body, such as atherosclerosis, arthritis, rheumatoid arthritis, pulmonary inflammation, neuronal degeneration, and cancer. Therefore, it is necessary to monitor and control the concentration of  $\text{ClO}^-$  in drinking water and in vivo. At present, a variety of detection methods have been developed for the determination of  $\text{ClO}^-$  such as colorimetric [5–8], fluorescent [1,9–11], luminescent [12], and electrochemical [13] methods. Since fluorescence methods usually have the advantages of high sensitivity and fast response, most of the reported analytical detection methods are fluorescent methods. Among these fluorescent methods, various nanomaterials have been widely used in fluorescence analysis because of their high luminous efficiency. Li and his co-researchers synthesized copper nanoclusters (Cu NCs) and applied them in the determination of hypochlorite ( $\text{ClO}^-$ ) [14]. Fang and his co-researchers utilized starch, boric acid, and L-3,4-dihydroxyphenylalanine (L-DOPA) to synthesize boric acid-protected gold nanoclusters and applied them in ratiometric fluorescent resonance energy transfer

(FRET) detection of  $\text{ClO}^-$  [15]. Liu and his co-researchers reported a facile microwave-assisted synthesis of  $\text{Ti}_3\text{C}_2$  MXene quantum dots for ratiometric fluorescence detection of hypochlorite [16]. Duan and his co-researchers reported a red fluorescent organic small molecule probe (S-BODIPY) for sensitive and specific imaging of  $\text{HClO}/\text{ClO}^-$  in vitro and in vivo. Wang and his co-researchers reported aminophenylboronic acid-functionalized N-doped carbon dots and applied them in selective detection of  $\text{ClO}^-$  [17]. Among these various materials for  $\text{ClO}^-$  detection, carbon quantum dots have attracted more and more researchers' attention because of their simple synthesis method and low toxicity.

Ratiometric fluorescent probes are a kind of fluorescent materials with two emission wavelengths. The intensity ratio of the two emission wavelengths is linear with the concentration of the targets [14,15,18]. Ratiometric fluorescence probes have the function of self-regulation and establish an internal standard, which can reduce the interference of other factors. Therefore, compared with ordinary fluorescent probes, ratiometric fluorescent probes have stronger anti-interference ability, higher sensitivity and selectivity, and have greater application potential in practical analysis [7,15,19–23]. Therefore, more and more researchers focus on the study of fluorescence ratiometric methods. For example, Huang and his partners designed a near-infrared ratiometric fluorescent probe based on ophorone and coumarin to detect  $\text{ClO}^-$  [22]. This probe has a red emission peak at 685 nm. It produces a blue emission peak at 486 nm in the presence of  $\text{ClO}^-$ . After the addition of  $\text{ClO}^-$ , fluorescence intensity at 468 nm gets increased and fluorescence intensity at 685 nm gets decreased. Therefore, fluorescent intensity ratio ( $F_{486\text{nm}}/F_{685\text{nm}}$ ) can be used to detect  $\text{ClO}^-$ . Sun and his co-researchers reported metal-organic frameworks (MOFs)-based ratiometric fluorescence strategy for  $\text{ClO}^-$  detection [21]. This fluorescent MOFs exhibited a dual fluorescence emission at 433 and 621 nm, and  $\text{ClO}^-$  can weaken blue fluorescence at 433 nm while fluorescence emission at 621 nm is kept stable. All of these methods are usually limited by the complex reaction and inconvenient operation to synthesize ratiometric fluorescent probes. Therefore, to explore facile and fast methods to prepare ratiometric fluorescent probes is of great importance.

As reported, phenylboronic acid bond is easy to bind to two o-phenolic hydroxyl groups to form phenyl borate ester bond [24]. Meanwhile  $\text{ClO}^-$  can oxidize phenyl borate ester bond [25,26]. Inspired by these results, a novel dopamine-functionalized carbon nanodot (C-dots) ratiometric fluorescence probe for the determination of hypochlorite ( $\text{ClO}^-$ ) is reported in this work (Scheme 1). Fluorescent C-dots synthesized via a hydrothermal procedure using 3-hydroxyphenylboronic acid exhibit maximal emission at 420 nm. After modified with dopamine, dopamine-functionalized C-dots have two maximal emissions at 420 nm and 460 nm. Fluorescent intensity at 460 nm gets quenched obviously with the addition of  $\text{ClO}^-$  while fluorescent intensity at 420 nm is almost unaffected. It is in accordance with typical ratiometric fluorescence probes with the function of self-regulation and an internal standard. Therefore, dopamine-functionalized C-dots are developed as ratiometric fluorescence probe for efficient and sensitive detection of  $\text{ClO}^-$ .



**Scheme 1.** Formation of dopamine-functionalized C-dots and its application in ratiometric fluorescence detection of  $\text{ClO}^-$ .

## 2. Experimental Section

### 2.1. Materials and Reagents

3-hydroxyphenylboric acid, hypochlorous acid, dopamine, and other inorganic salts are purchased from alighting reagent company (Shanghai, China). Doubly distilled water was used throughout all experiments.

### 2.2. Instrumentation

Fluorescent spectra were recorded on Perkin Elmer LS55 and F90 fluorescence spectrophotometer (Lengguang Technology Co., Ltd, Shanghai, China). Photos were taken under 365 nm ultraviolet light using ZF-20D ultraviolet analysis equipment from Gongyi Yuhua Instrument Co., Ltd. (Gongyi, China). S-25 digital pH meter (Shanghai Jing ke Industry Company, Shanghai, China) is used to detect the acidity of solutions.

### 2.3. Synthesis of C-Dots

First, 0.2 g 3-hydroxyphenylboric acid was dissolved in 20 mL water. pH was adjusted to pH 9.0 with 0.1 M NaOH and stirred for 5 min. Then it was bubbled with nitrogen for 1 h to remove oxygen. Finally, it was loaded into autoclave for hydrothermal reaction at 160 °C for 8 h. After cooling to room temperature, the reacted solution was centrifuged at 10,000 rpm for 30 min, and the supernatant was taken and stored at 4 °C.

### 2.4. Synthesis of Dopamine-Functionalized C-Dots

A total of 200 µL C-dots, 150 µL 5 mM dopamine, and 450 mL water were added to a 1.5 mL centrifuge tube, which has 200 µL 0.2 M phosphate buffer pH 8.0. The whole volume of the mixture solution was 1.0 mL. After reacting at 25 °C for 5 min, dopamine-functionalized C-dots were obtained.

### 2.5. Procedures of Fluorescent “Turn-Off” Detection of ClO<sup>-</sup>

A total of 20 µL dopamine-functionalized C-dots, 200 µL 0.2 M phosphate buffer pH 8.0, and different concentrations of ClO<sup>-</sup> solution were added to a 1.5 mL centrifuge tube and mixed thoroughly. The final volume was kept at 1.0 mL. They were used to detect fluorescence after 5 min.

### 2.6. Fluorescent Detection of ClO<sup>-</sup> in Tap Water Samples

Real tap water samples were directly collected from our laboratory in Chongqing normal university. Then 500 µL tap water was added to 200 µL 0.2 M phosphate buffer solution (pH 8.0). Other procedures were kept the same as the above procedures of fluorescent “turn-off” detection of ClO<sup>-</sup>. To check the accuracy of this method, three different concentrations of ClO<sup>-</sup> (5 µM, 20 µM, and 50 µM) were used to obtain recovery via recovery methods of standard additions.

## 3. Results and Discussion

### 3.1. Characteristics of Dopamine-Functionalized C-Dots

Fluorescence intensity of phenylboric acid with different groups was investigated. As shown in Figure 1A, five phenylboric acid compounds are utilized as carbon sources to synthesize C-dots. They are 3-hydroxyphenylboric acid with hydroxyl group, 3-aminophenylboric acid with amino group, 4-formylphenylboronic acid with formyl group, 4-mercaptophenylboronic acid with thiol group, and 4-vinyl phenylboronic acid with vinyl group. For 4-mercaptophenylboronic acid and 4-vinyl phenylboronic acid, nearly no fluorescent C-dots are obtained after a hydrothermal process. It suggests that thiol group or vinyl group may quench the fluorescence. Since C-dots prepared with 3-hydroxyphenylboric acid have the highest luminescence intensity, C-dots prepared with 3-hydroxyphenylboric acid are applied in modification with dopamine in order to obtain ratiometric fluorescence probe of dopamine-functionalized C-dots.

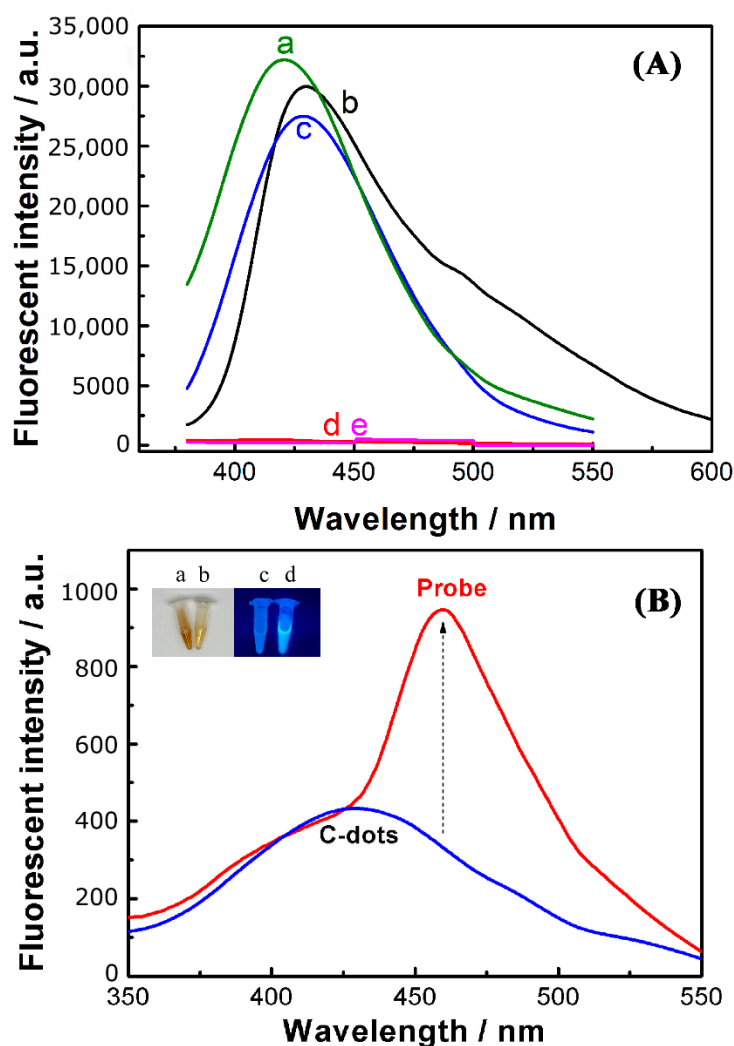


**Figure 1.** Fluorescence of C-dots synthesized using difference reagents (A). 3-hydroxyphenylboronic acid (curve a); 3-aminophenylboronic acid (curve b); 4-formylphenylboronic acid (curve c); 4-mercaptophenylboronic acid (curve d); 4-vinyl phenylboronic acid (curve e). Fluorescence spectra of C-dots using 3-hydroxyphenylboronic acid and dopamine-functionalized fluorescent C-dots (probe) (B). The inserted two photos show the color of C-dots (a) and dopamine-functionalized fluorescent C-dots (b) solutions.  $\lambda_{\text{ex}}$ : 285 nm. The other two inserted photos show fluorescence color of C-dots (c) and dopamine-functionalized fluorescent C-dots (d) solutions under 365 nm ultraviolet light.

As shown in Figure 1B, the synthesized C-dots have a dark brown transparent solution and emit blue fluorescence under 365 nm ultraviolet light (the inserted photos). The synthesized C-dots have maximal fluorescence emission at 420 nm. After C-dots modification with dopamine, dopamine-functionalized C-dots as the ratiometric fluorescence probe are changed from dark brown to brown yellow transparent solution (the inserted photos). Moreover, fluorescence of dopamine-functionalized C-dots gets significantly stronger than that of C-dots. More importantly, dopamine-functionalized C-dots have two fluorescence emission peaks at 420 nm and 460 nm at maximal excitation wavelength of 285 nm (Figure 2A) with fluorescence quantum yield (QY) of 28.4%. Moreover, dopamine-functionalized C-dots can be stable within two months by monitoring the fluorescent intensity, which suggests their good photostability (Figure 3). From TEM images (Figure 2B), it can be seen that dopamine-functionalized C-dots are nearly 1–2 nm, which is nearly the same as C-dots in most other reports [27]. It is utilized as fluorescent probe for ratiometric detection of  $\text{ClO}^-$  in the following experiment.

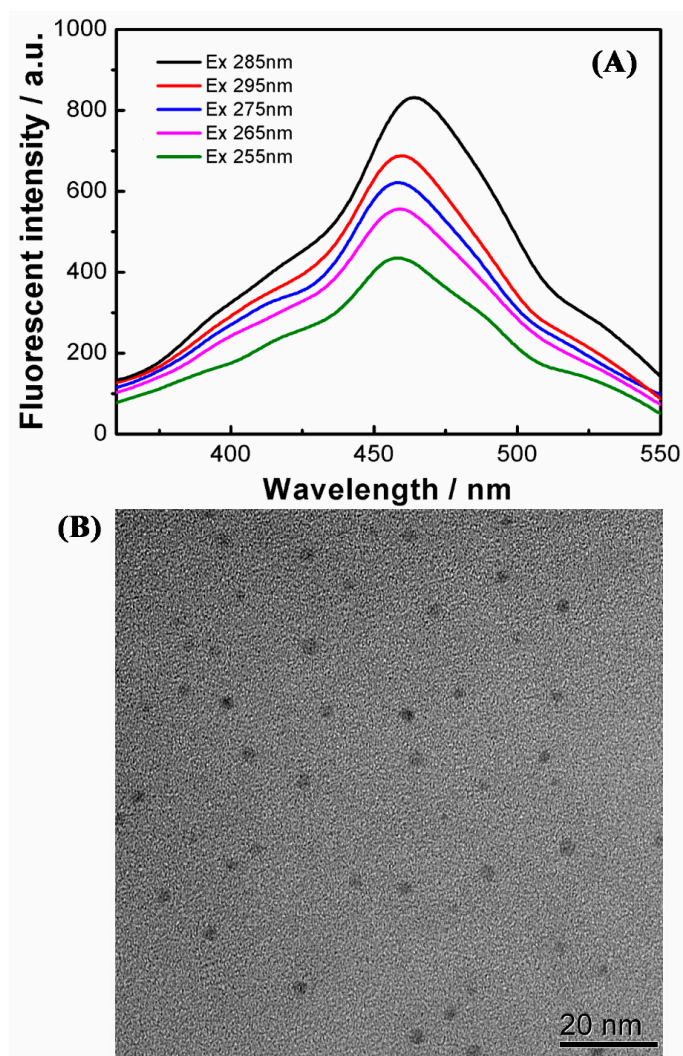


**Figure 2.** Fluorescence properties (A) and TEM image (B) of dopamine-functionalized fluorescent C-dots under difference excitation wavelength from 255 nm to 295 nm.

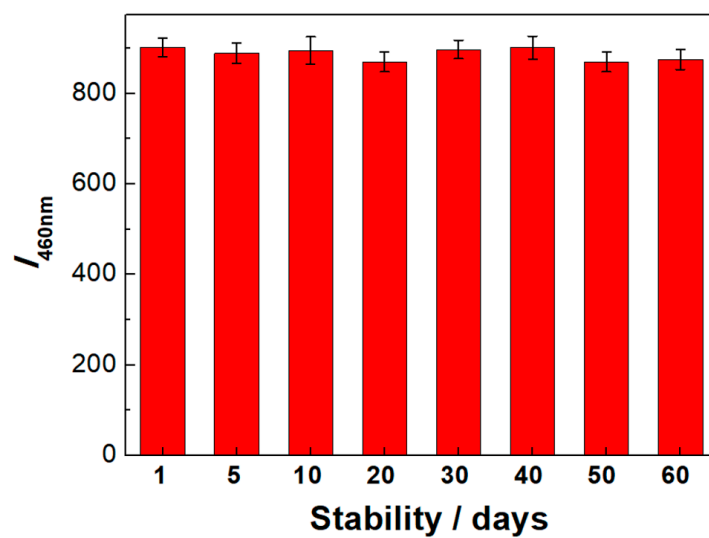


**Figure 3.** Fluorescent intensity at 460 nm ( $J_{460nm}$ ) of dopamine-functionalized fluorescent C-dots within two months.  $\lambda_{ex}$ : 285 nm.

### 3.2. The Feasibility of $\text{ClO}^-$ Detection Using Dopamine-Functionalized Fluorescent C-Dots

As shown in Figure 4, fluorescent intensity of the probe at 460 nm gets decreased nearly 56% after adding  $\text{ClO}^-$ . Fluorescent intensity at 420 nm is almost unaffected, which can be used as a reference to improve the detection sensitivity and selectivity. Therefore, it indicates that dopamine-functionalized C-dots are feasible to be applied as ratiometric fluorescent probe to detect  $\text{ClO}^-$ .

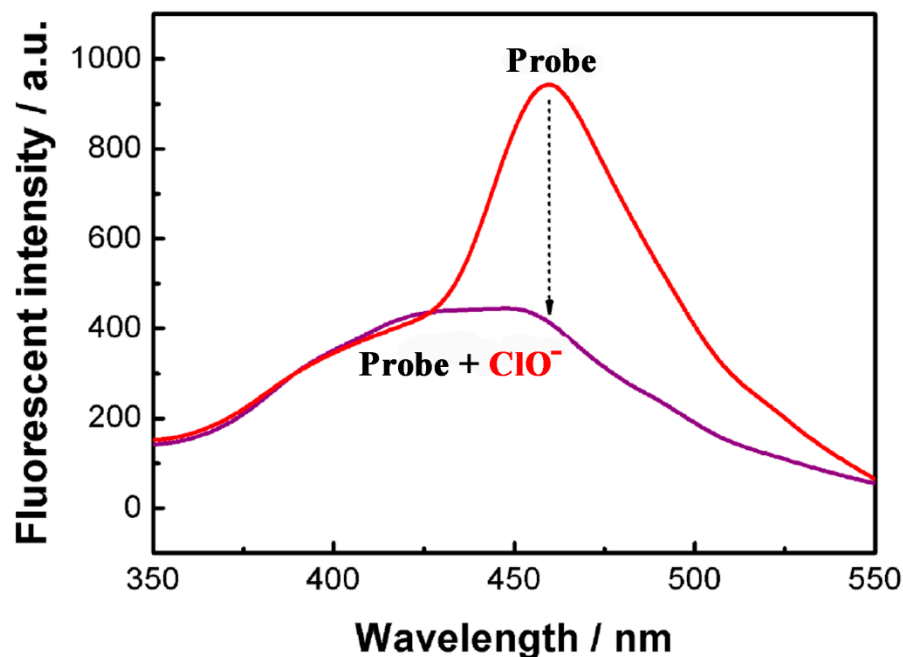


**Figure 4.** Fluorescence spectrum of the probe (red line); fluorescence spectrum of the probe in the presence of  $\text{ClO}^-$  (purple line).  $c(\text{probe}, \mu\text{L})$ : 20;  $c(\text{ClO}^-, \mu\text{M})$ : 50; 40 mM phosphate buffer solution: pH 8.0; temperature ( $^{\circ}\text{C}$ ): 25 (room temperature); reaction time (minutes): 5;  $\lambda_{\text{ex}}$ : 285 nm;  $\lambda_{\text{em}}$ : 420 nm, 460 nm.

According to UV-Vis absorption spectra results (Figure 5), the possible mechanism of fluorescence enhancement at 460 nm after dopamine modification is speculated that C-dots have phenylboronic acid group on the surface of nanoparticles. Dopamine may react with phenylboronic acid group to form phenyl borate ester bond [9,15,28], which not only enhances the fluorescence but also brings a new absorption peak at 420 nm. After the addition of  $\text{ClO}^-$ , phenyl borate ester bond is oxidized by  $\text{ClO}^-$  to form phenolic hydroxyl group. The oxidation of other borate ester bond by  $\text{ClO}^-$  has been reported by some researchers [11,17,22,27]. Moreover, UV-Vis absorption spectra can also show that the new absorption peak at 420 nm is decreased obviously after the addition of  $\text{ClO}^-$ . Therefore, fluorescent quenching effect of  $\text{ClO}^-$  to dopamine-functionalized C-dots may be also ascribed to oxidation of phenyl borate ester bond by  $\text{ClO}^-$ .

### 3.3. The Optimization of $\text{ClO}^-$ Detection

To improve the sensitivity of  $\text{ClO}^-$  detection, pH and temperature are investigated. With the increasing of pH values from 4.4 to 9.0, fluorescent intensity at 420 nm is almost unaffected. As shown in Figure 6, fluorescent intensity at 460 nm in the absence of  $\text{ClO}^-$  has no obvious changes from pH 4.4 to 7.4 and then gets enhanced greatly at pH 8.0 and 9.0. While in the presence of  $\text{ClO}^-$ , fluorescent intensity at 460 nm is kept at stable low value from pH 4.4 to 9.0. Therefore, fluorescence quenching effect after the addition of  $\text{ClO}^-$  gets enhanced at pH 8.0 and 9.0. In suggests that the oxidation of borate ester bond by  $\text{ClO}^-$  needs weak alkaline conditions. Therefore, to obtain the stable and maximum quenching

effect, pH 8.0 is selected as the best condition for  $\text{ClO}^-$  detection. It is also conducive to detecting  $\text{ClO}^-$  in actual samples.

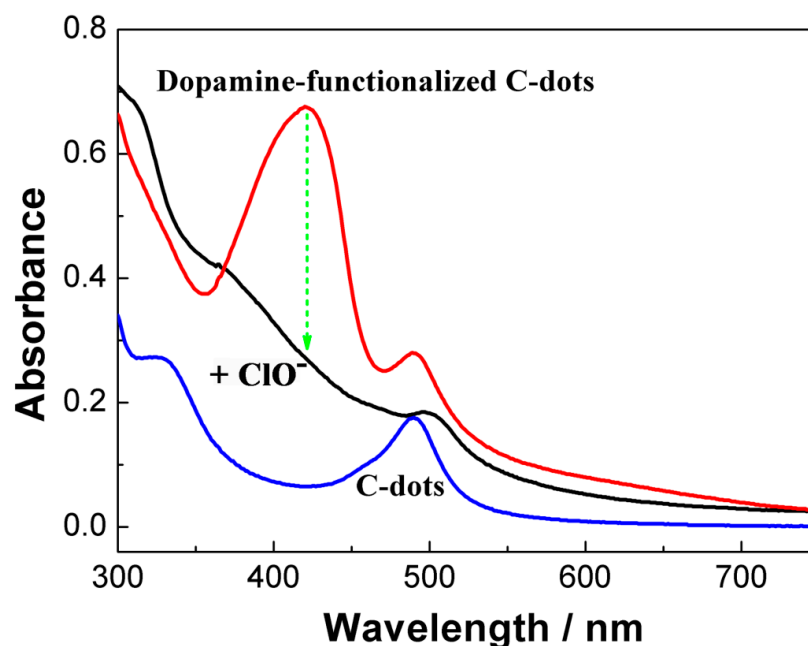


**Figure 5.** UV-Vis absorption spectra of C-dots, dopamine-functionalized C-dots before and after the addition of  $\text{ClO}^-$ .

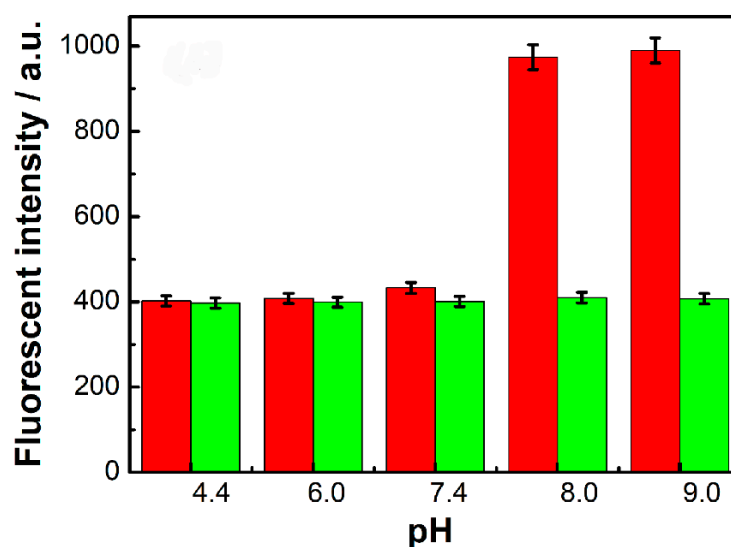


**Figure 6.** The effect of pH on the detection of  $\text{ClO}^-$ . Red columns represent the fluorescence intensity of the probe; green columns represent the fluorescence intensity of the mixed solution after adding  $\text{ClO}^-$ .  $c(\text{probe}, \mu\text{L})$ : 20;  $c(\text{ClO}^-, \mu\text{M})$ : 50; 40 mM phosphate buffer solution: pH 8.0.  $\lambda_{\text{ex}}$ : 285 nm;  $\lambda_{\text{em}}$ : 460 nm; all the error bars represent the standard deviation of three measurements.

Three different temperatures of 25 °C (room temperature), 37 °C, and 50 °C are utilized to investigate its effect on  $\text{ClO}^-$  detection (Supporting Information, Figure S1). Fluorescence quenching effect of  $\text{ClO}^-$  on the probe nearly has no relation with the increasing temperature. It suggests that temperature has nearly no effect on  $\text{ClO}^-$  detection, which is conducive to obtain stable quenching effect in  $\text{ClO}^-$  detection. To achieve a facile and stable fluorescent quenching effect, the optimum temperature is 25 °C (room temperature) for  $\text{ClO}^-$  detection.

The kinetic behavior of  $\text{ClO}^-$  detection is also investigated in Figure S2 (Supporting Information) and measured via “time scan mode” in fluorescence spectrophotometer. When time is changed from immediately to 250 s, fluorescent intensity of the probe is stable. Moreover, fluorescent intensity of the probe after the addition of  $\text{ClO}^-$  is kept at a stable low value. It indicates that fluorescent quenching effect of the probe by  $\text{ClO}^-$  can be completed immediately. Fluorescent detection of  $\text{ClO}^-$  is a fast process within several seconds. It is conducive to fast detect  $\text{ClO}^-$  in our daily life or some emergency detection occasions. To reach a fast and stable fluorescent quenching effect for  $\text{ClO}^-$  detection, 5 min is chosen as the optimized condition for  $\text{ClO}^-$  detection.

### 3.4. The Sensitivity and Selectivity of $\text{ClO}^-$ Detection

The effects of different concentrations of  $\text{ClO}^-$  on fluorescent probes are studied under the optimal experimental conditions. As shown in Figure 7A, fluorescent intensity of this ratiometric fluorescence probe at 460 nm gets decreased gradually with the increasing concentration of  $\text{ClO}^-$  from 2  $\mu\text{M}$  to 60  $\mu\text{M}$ . Fluorescent intensity at 420 nm is almost unaffected. The ratio of fluorescent intensity at 460 nm and 420 nm ( $I_{460\text{nm}}/I_{420\text{nm}}$ ) has linear relationship ( $r = 0.9906$ ) with the concentration of  $\text{ClO}^-$  from 2  $\mu\text{M}$  to 60  $\mu\text{M}$  (Figure 7B) and the limit of detection (LOD) of 0.6  $\mu\text{M}$ . Compared with other methods (Table 1), this method has high sensitivity.

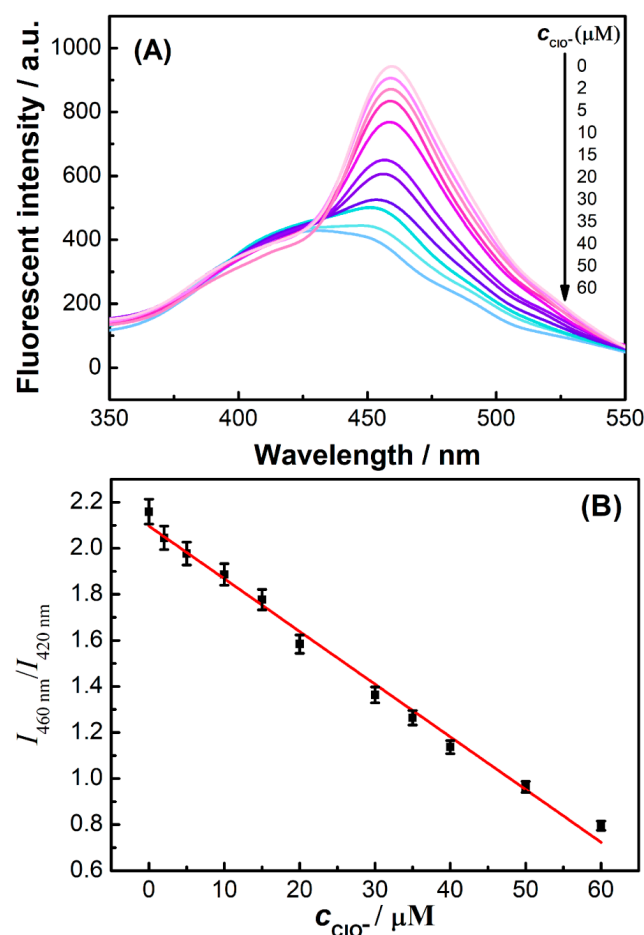


**Figure 7.** Fluorescence spectra (A) and linear calibration diagram (B).  $c(\text{ClO}^-)$ ,  $\mu\text{M}$ : 0, 2, 5, 10, 15, 20, 30, 35, 40, 50, 60;  $c(\text{probe}, \mu\text{L})$ : 20; reaction time (min): 5; temperature ( $^{\circ}\text{C}$ ): 25 (room temperature); 40 mM phosphate buffer solution: pH 8.0.  $\lambda_{\text{ex}}$ : 285 nm;  $\lambda_{\text{em}}$ : 460 nm. All the error bars represent the standard deviation of the three measurements.

**Table 1.** Comparison of different methods for  $\text{ClO}^-$  detection.

Method	Linear Range ( $\mu\text{M}$ )	LOD ( $\mu\text{M}$ )	Refs
Colorimetry	5–200	2.2	[6]
Colorimetry	0.17–1.54	0.2	[8]
Fluorescence	0–200	6.8	[10]
Fluorescence	\	4.2	[29]
Fluorescence	1–5	0.2	[30]
Fluorescence	2–16	2.0	[31]
Fluorescence	25–150	5.0	[16]
Fluorescence	0–412	24	[14]
Ratiometric fluorescence	0.05–7	0.01	[5]
Ratiometric fluorescence	2–60	0.6	This work

The selectivity of the probe used in  $\text{ClO}^-$  detection is also investigated in Figure 8. The same concentrations of  $\text{ClO}^-$ ,  $\text{SO}_4^{2-}$ ,  $\text{Cl}^-$ ,  $\text{NO}_3^-$ ,  $\text{S}^{2-}$ ,  $\text{CO}_3^{2-}$ ,  $\text{Mg}^{2+}$ ,  $\text{Ba}^{2+}$ ,  $\text{Ag}^+$ ,  $\text{Fe}^{3+}$ ,  $\text{Ca}^{2+}$ ,  $\text{Na}^+$ ,  $\text{Cr}^{6+}$ ,  $\text{Cr}^{3+}$ ,  $\text{Hg}^+$ ,  $\text{H}_2\text{O}_2$ , glutamate, cysteine, and citric acid were compared to  $\text{ClO}^-$ . Only  $\text{ClO}^-$  had obvious fluorescence quenching effect on this probe. Therefore, this method has good selectivity for the detection of  $\text{ClO}^-$ .

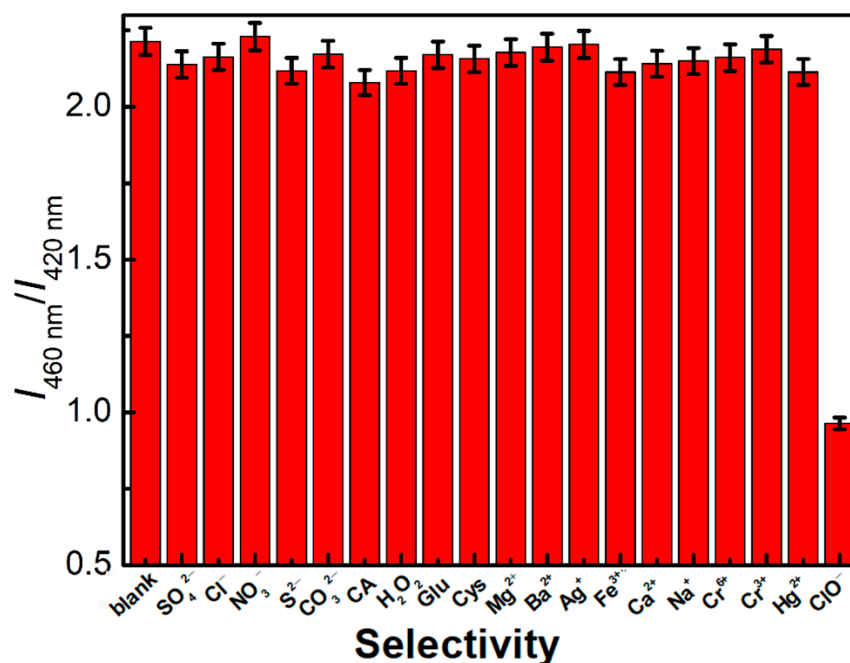


**Figure 8.** The selectivity of this probe in  $\text{ClO}^-$  detection toward other substances. The concentrations of  $\text{ClO}^-$ ,  $\text{SO}_4^{2-}$ ,  $\text{Cl}^-$ ,  $\text{NO}_3^-$ ,  $\text{S}^{2-}$ ,  $\text{CO}_3^{2-}$ ,  $\text{Mg}^{2+}$ ,  $\text{Ba}^{2+}$ ,  $\text{Ag}^+$ ,  $\text{Fe}^{3+}$ ,  $\text{Ca}^{2+}$ ,  $\text{Na}^+$ ,  $\text{Cr}^{6+}$ ,  $\text{Cr}^{3+}$ ,  $\text{Hg}^+$ ,  $\text{H}_2\text{O}_2$ , Glu (glutamate), Cys (cysteine), and CA (citric acid) are  $50 \mu\text{M}$ ;  $c(\text{probe}, \mu\text{L})$ : 20; reaction time (min): 5; temperature ( $^\circ\text{C}$ ): 25 (room temperature); 40 mM phosphate buffer solution: pH 8.0.  $\lambda_{\text{ex}}$ : 285 nm;  $\lambda_{\text{em}}$ : 460 nm. All error bars represent the standard deviation of the three measurements.

### 3.5. Fluorescent Detection of $\text{ClO}^-$ in Tap Water Samples

Similarly like most fluorescent detection reports [6,21,32], the standard addition method is mostly applied to detect  $\text{ClO}^-$  in tap water in order to check the accuracy and potential application of the present method. Tap water samples are obtained in our laboratory in Chongqing Normal University. As shown in Table 2, the average recoveries of  $\text{ClO}^-$  in tap water samples are from 95.7% to 103.2% with the relative standard deviations (RSDs) lower than 5%. It indicates that this ratiometric fluorescent method for detection of  $\text{ClO}^-$  is suitable in real water samples.

**Table 2.** Determination of  $\text{ClO}^-$  in tap water.

Samples	Added ( $\mu\text{M}$ )	Found ( $\mu\text{M}$ , $n = 3$ )	Recoveries (% , $n = 3$ )
1	5	8.54, 8.40, 8.46	$95.7 \pm 1.4$
2	20	24.01, 23.94, 25.05	$103.2 \pm 3.1$
3	50	51.92, 52.57, 54.41	$98.6 \pm 2.6$

The concentration of  $\text{ClO}^-$  in tap water is  $3.68 \mu\text{M}$

#### 4. Conclusions

To sum up, a novel ratiometric fluorescence probe of dopamine-functionalized carbon nanodots is synthesized in this study. Fluorescent C-dots with maximal emission at 420 nm are synthesized via a hydrothermal synthesis of 3-hydroxyphenylboric acid and then modified with dopamine to form dopamine-functionalized C-dots, which have two maximal emissions at 420 nm and 460 nm. Fluorescent intensity at 460 nm gets quenched obviously with the addition of  $\text{ClO}^-$  and fluorescent intensity at 420 nm is almost unaffected. Fluorescent intensity at 420 nm can be used as a reference to improve the detection sensitivity and selectivity. Therefore dopamine-functionalized C-dots can be used as a ratiometric fluorescence probe for highly sensitive detection of  $\text{ClO}^-$ . The possible mechanism of fluorescence enhancement at 460 nm after dopamine modification may be ascribed to the formation of phenyl borate ester bond. Moreover, oxidization of other borate ester bonds by  $\text{ClO}^-$  may quench the fluorescence of dopamine-functionalized C-dots. This fluorescent probe has good water solubility and shows high selectivity for the detection of  $\text{ClO}^-$  toward other anions ( $\text{SO}_4^{2-}$ ,  $\text{Cl}^-$ ,  $\text{NO}_3^-$ ,  $\text{S}^{2-}$ ,  $\text{CO}_3^{2-}$ ), metal ions ( $\text{Mg}^{2+}$ ,  $\text{Ba}^{2+}$ ,  $\text{Ag}^+$ ,  $\text{Fe}^{3+}$ ,  $\text{Ca}^{2+}$ ,  $\text{Na}^+$ ,  $\text{Cr}^{6+}$ ,  $\text{Cr}^{3+}$ ,  $\text{Hg}^+$ ), or other substances such as  $\text{H}_2\text{O}_2$ , glutamate, cysteine, and citric acid. When it is utilized in  $\text{ClO}^-$  detection in tap water, the average recoveries are from 95.7% to 103.2%. Therefore, it has great development potential in the detection of  $\text{ClO}^-$  in real water.

**Supplementary Materials:** The following supporting information can be downloaded at: <https://www.mdpi.com/article/10.3390/chemosensors10100383/s1>. Figure S1: the effect of temperature on the detection of  $\text{ClO}^-$ ; Figure S2: kinetic behavior of  $\text{ClO}^-$  detection.

**Author Contributions:** Conceptualization, L.C. and W.Q.; data curation, L.C. and C.D.; formal analysis, L.C., C.D. and Y.W.; funding acquisition, W.Q.; investigation, L.C., C.D. and Y.W.; methodology, L.C.; project administration, W.Q.; software, L.C.; supervision, W.Q.; validation, C.D. and Y.W.; visualization, C.D. and Y.W.; writing—original draft, L.C.; writing—review and editing, W.Q. All authors have read and agreed to the published version of the manuscript.

**Funding:** This work was supported by the Scientific and Technological Research Program of Chongqing Education Committee (No. KJQN201900521), the Program for Top-Notch Young Innovative Talents of Chongqing Normal University (No. 02030307-00042) and the Innovation and Entrepreneurship Team of Inorganic Optoelectronic Functional Materials for Chongqing Yingcai (No. cstc2021ycjh-bgzxm0131).

**Institutional Review Board Statement:** Not applicable.

**Informed Consent Statement:** Not applicable.

**Data Availability Statement:** Not applicable.

**Acknowledgments:** The authors would like to thank Chongqing Key Laboratory of Inorganic Functional Materials (Chongqing Normal University) at Chongqing for supporting this research and providing the appropriate research environment.

**Conflicts of Interest:** The authors declare no conflict of interest.

#### References

- Chen, P.; Zheng, Z.; Zhu, Y.; Dong, Y.; Wang, F.; Liang, G. Bioluminescent turn-on probe for sensing hypochlorite in vitro and in tumors. *Anal. Chem.* **2017**, *89*, 5693–5696. [[CrossRef](#)] [[PubMed](#)]

2. Lin, Y.-S.; Chuang, L.-W.; Lin, Y.-F.; Hu, S.-R.; Huang, C.-C.; Huang, Y.-F.; Chang, H.-T. Development of fluorescent carbon nanoparticle-based probes for intracellular pH and hypochlorite sensing. *Chemosensors*. **2022**, *10*, 64. [[CrossRef](#)]
3. Lee, M.; Choe, D.; Park, S.; Kim, H.; Jeong, S.; Kim, K.-T.; Kim, C. A novel thiosemicarbazide-based fluorescent chemosensor for hypochlorite in near-perfect aqueous solution and zebrafish. *Chemosensors* **2021**, *9*, 65. [[CrossRef](#)]
4. Shiraiishi, Y.; Nakatani, R.; Takagi, S.; Yamada, C.; Hirai, T. A naphthalimide–sulfonylhydrazine conjugate as a fluorescent chemodosimeter for hypochlorite. *Chemosensors* **2020**, *8*, 123. [[CrossRef](#)]
5. Zhan, Y.; Luo, F.; Guo, L.; Qiu, B.; Lin, Y.; Li, J.; Chen, G.; Lin, Z. Preparation of an efficient ratiometric fluorescent nanoprobe (m-CDs@[Ru(bpy)<sub>3</sub>]<sup>2+</sup>) for visual and specific detection of hypochlorite on site and in living cells. *ACS Sens.* **2017**, *2*, 1684–1691. [[CrossRef](#)]
6. Wei, Z.; Li, H.; Liu, S.; Wang, W.; Chen, H.; Xiao, L.; Ren, C.; Chen, X. Carbon dots as fluorescent/colorimetric probes for real-time detection of hypochlorite and ascorbic acid in cells and body fluid. *Anal. Chem.* **2019**, *91*, 15477–15483. [[CrossRef](#)]
7. Li, Y.; Liu, L.; Tang, Y.; Wang, Y.; Han, J.; Ni, L. A new colorimetric and ratiometric probe for highly selective recognition and bioimaging of ClO<sup>-</sup> and Al(3). *Spectrochim. Acta. A* **2020**, *232*, 118154. [[CrossRef](#)]
8. Wang, X.; Tang, H.; Tian, X.; Zeng, R.; Jia, Z.; Huang, X. Sunlight and UV driven synthesis of Ag nanoparticles for fluorometric and colorimetric dual-mode sensing of ClO<sup>-</sup>. *Spectrochim. Acta. A* **2020**, *229*, 117996. [[CrossRef](#)]
9. Li, M.-Y.; Li, K.; Liu, Y.-H.; Zhang, H.; Yu, K.-K.; Liu, X.; Yu, X.-Q. Mitochondria-immobilized fluorescent probe for the detection of hypochlorite in living cells, tissues, and zebrafishes. *Anal. Chem.* **2020**, *92*, 3262–3269. [[CrossRef](#)]
10. Wang, L.; Li, B.; Jiang, C.; Sun, R.; Hu, P.; Chen, S.; Wu, W. A bodipy based fluorescent probe for the rapid detection of hypochlorite. *J. Fluoresc.* **2018**, *28*, 933–941. [[CrossRef](#)]
11. Du, Y.; Wang, B.; Jin, D.; Li, M.; Li, Y.; Yan, X.; Zhou, X.; Chen, L. Dual-site fluorescent probe for multi-response detection of ClO<sup>-</sup> and H<sub>2</sub>O<sub>2</sub> and bio-imaging. *Anal. Chim. Acta.* **2020**, *1103*, 174–182. [[CrossRef](#)]
12. Fu, X.; Wu, J.; Xu, H.; Wan, P.; Fu, H.; Mei, Q. Luminescence nanoprobe in the near-infrared-II window for ultrasensitive detection of hypochlorite. *Anal. Chem.* **2021**, *93*, 15696–15702. [[CrossRef](#)]
13. Dong, H.; Zhou, Y.; Zhao, L.; Hao, Y.; Zhang, Y.; Ye, B.; Xu, M. Dual-response ratiometric electrochemical microsensor for effective simultaneous monitoring of hypochlorous acid and ascorbic acid in human body fluids. *Anal. Chem.* **2020**, *92*, 15079–15086. [[CrossRef](#)]
14. Li, Y.; He, Y.; Ge, Y.; Song, G.; Zhou, J. Smartphone-assisted visual ratio-fluorescence detection of hypochlorite based on copper nanoclusters. *Spectrochim. Acta. A* **2021**, *255*, 119740. [[CrossRef](#)]
15. Fang, H.; Yu, H.; Lu, Q.; Fang, X.; Zhang, Q.; Zhang, J.; Zhu, L.; Ma, Q. A new ratiometric fluorescent probe for specific monitoring of hROS under physiological conditions using boric acid-protected l-dopa gold nanoclusters. *Anal. Chem.* **2020**, *92*, 12825–12832. [[CrossRef](#)]
16. Liu, M.; Bai, Y.; He, Y.; Zhou, J.; Ge, Y.; Zhou, J.; Song, G. Facile microwave-assisted synthesis of Ti<sub>3</sub>C<sub>2</sub> MXene quantum dots for ratiometric fluorescence detection of hypochlorite. *Microchim. Acta.* **2021**, *188*, 15. [[CrossRef](#)]
17. Wang, L.L.; Jana, J.; Chung, J.S.; Hur, S.H. High quantum yield aminophenylboronic acid-functionalized N-doped carbon dots for highly selective hypochlorite ion detection. *Spectrochim. Acta. A* **2021**, *260*, 119895. [[CrossRef](#)]
18. Shen, S.-L.; Zhang, X.-F.; Ge, Y.-Q.; Zhu, Y.; Cao, X.-Q. A novel ratiometric fluorescent probe for the detection of HOCl based on FRET strategy. *Sens. Actuat. B Chem.* **2018**, *254*, 736–741. [[CrossRef](#)]
19. Chu, H.; Yao, D.; Chen, J.; Yu, M.; Su, L. Detection of Hg<sup>2+</sup> by a Dual-Fluorescence Ratio Probe Constructed with Rare-Earth-Element-Doped Cadmium Telluride Quantum Dots and Fluorescent Carbon Dots. *ACS Omega* **2021**, *6*, 10735–10744. [[CrossRef](#)]
20. Duan, C.; Won, M.; Verwilt, P.; Xu, J.; Kim, H.S.; Zeng, L.; Kim, J.S. In vivo imaging of endogenously produced HClO in zebrafish and mice using a bright, photostable ratiometric fluorescent probe. *Anal. Chem.* **2019**, *91*, 4172–4178. [[CrossRef](#)]
21. Sun, Y.-Q.; Cheng, Y.; Yin, X.-B. Dual-ligand lanthanide metal–organic framework for sensitive ratiometric fluorescence detection of hypochlorous acid. *Anal. Chem.* **2021**, *93*, 3559–3566. [[CrossRef](#)]
22. Huang, Y.; Zhang, Y.; Huo, F.; Chao, J.; Yin, C. A near-infrared ratiometric fluorescent probe with large stokes based on isophorone for rapid detection of ClO<sup>-</sup> and its bioimaging in cell and mice. *Sens. Actuat. B Chem.* **2019**, *287*, 453–458. [[CrossRef](#)]
23. Yang, X.; Qin, X.; Zhu, F.; Shi, W. A through-bond energy transfer-based ratiometric fluorescent pH probe: For extreme acidity and extreme alkaline detection with large emission shifts. *Talanta* **2019**, *200*, 350–356. [[CrossRef](#)]
24. Fabre, B.; Hauquier, F. Boronic acid-functionalized oxide-free silicon surfaces for the electrochemical sensing of dopamine. *Langmuir* **2017**, *33*, 8693–8699. [[CrossRef](#)]
25. Wang, Q.; Liu, C.; Chang, J.J.; Lu, Y.; He, S.; Zhao, L.C.; Zeng, X.S. Novel water soluble styrylquinolinium boronic acid as a ratiometric reagent for the rapid detection of hypochlorite ion. *Dyes Pigm.* **2013**, *99*, 733–739. [[CrossRef](#)]
26. Shi, W.-J.; Huang, Y.; Liu, W.; Xu, D.; Chen, S.-T.; Liu, F.; Hu, J.; Zheng, L.; Chen, K. A BODIPY-based “OFF-ON” fluorescent probe for fast and selective detection of hypochlorite in living cells. *Dyes Pigm.* **2019**, *170*, 107566. [[CrossRef](#)]
27. Shen, P.; Xia, Y. Synthesis-modification integration: One-step fabrication of boronic acid functionalized carbon dots for fluorescent blood sugar sensing. *Anal. Chem.* **2014**, *86*, 5323–5329. [[CrossRef](#)] [[PubMed](#)]
28. Zhou, Z.; Zhang, M.; Liu, Y.; Li, C.; Zhang, Q.; Oupicky, D.; Sun, M. Reversible covalent cross-linked polycations with enhanced stability and ATP-responsive behavior for improved siRNA delivery. *Biomacromolecules* **2018**, *19*, 3776–3787. [[CrossRef](#)] [[PubMed](#)]
29. Kim, P.A.; Choe, D.; So, H.; Park, S.; Suh, B.; Jeong, S.; Kim, K.-T.; Kim, C.; Harrison, R.G. A selective fluorescence sensor for hypochlorite used for the detection of hypochlorite in zebrafish. *Spectrochim. Acta A* **2021**, *261*, 120059. [[CrossRef](#)] [[PubMed](#)]

30. Taheri, M.; Mansour, N. Functionalized silicon nanoparticles as fluorescent probe for detection of hypochlorite in water. *J. Photochem. Photobiol. A* **2019**, *382*, 111906. [[CrossRef](#)]
31. Wu, H.; Zhang, W.; Wu, Y.; Liu, N.; Meng, F.; Xie, Y.; Yan, L. A 7-diethylaminocoumarin-based chemosensor with barbituric acid for hypochlorite and hydrazine. *Microchem. J.* **2020**, *159*, 105461. [[CrossRef](#)]
32. Zhao, D.; Huang, Y.; Shi, B.; Li, S.; Zhao, S. Facile Fluorescent Differentiation of Aminophenol Isomers Based on Ce-Doped Carbon Dots. *ACS Sustain. Chem. Eng.* **2021**, *9*, 8136–8141. [[CrossRef](#)]